Quantification of structural uncertainties in the $k-\omega$ turbulence model

By Q. Wang† AND E. A. Dow†

We propose a method for building a statistical model for the structural uncertainties in the $k-\omega$ turbulence model. An inverse RANS problem is solved for a collection of randomly generated geometries to determine the turbulent viscosity that produces the flow field closest to that predicted by direct numerical simulation (DNS). A statistical model of the uncertainty in the turbulent viscosity calculated using the $k-\omega$ model is then developed using the data generated from solving the inverse problem. We present results for turbulent flow in a straight channel, as well as the preliminary results for the collection of randomly generated geometries.

1. Introduction

Despite its popularity, the flow field calculated using RANS simulations can contain significant uncertainty. In a RANS simulation, the effect of the unresolved turbulence on the statistically averaged flow field is represented by the Reynolds stress tensor. The value of the Reynolds stress depends on unresolved components of the flow field, and therefore can only be estimated by a RANS turbulence model. The most common class of RANS models, Boussinesq turbulent viscosity models, approximate the Reynolds stress tensor as an additional turbulent viscosity acting on the mean flow field. The uncertainties resulting from these inexact estimates are called model uncertainties or structural uncertainties in RANS simulations of turbulent flows.

These structural uncertainties often produce a significant contribution to the uncertainties in the flow fields calculated using RANS simulations, especially when the geometry in the flow is not clean, or when the flow experiences or is close to separation. For example, the performance of an airplane in landing and take-off configurations, as well as the performance of a turbine engine near stall, cannot be predicted confidently using RANS simulations due to the structural uncertainties inherent in RANS turbulence models.

2. Background

Due to its engineering importance, the uncertainties in RANS solutions of turbulent flows have been widely investigated. Most previous work focuses on characterizing the numerical errors, including those resulting from near wall grid spacing, grid stretching and numerical dissipation (Vaughn 2007; Davis 2004). Parametric and geometric uncertainties in RANS simulations have also been extensively studied (Loeven 2009; Witteveen 2009). Validation of RANS simulations against experimental results has been performed for a variety of applications, such as multi-element high-lift airfoils (Wild 2002). These studies have enabled a better understanding of the uncertainties present in RANS solutions through a posteriori analysis. However, in order to estimate uncertainties in RANS

† Department of Aeronautics and Astronautics, Massachusetts Institute of Technology

solutions of new engineering designs, a predictive method for quantifying the structural uncertainties is still needed.

A recent work by Oliver and Moser (Oliver 2009) presents one of the first attempts at quantifying structural uncertainties in RANS simulations. In their method, the tuning parameters in the Spalart-Allmaras RANS model are treated as random variables. The probability distributions of these tuning parameters are calculated by solving a Bayesian inverse problem based on experimental calibration data. Gaussian noise is added to the random model parameters on the state level. The magnitude and correlation length of this noise is estimated by solving a separate Bayesian inverse problem. The uncertainties in the RANS solution estimated using this method are shown to agree with the calibration data. Their method can also be generalized to other RANS turbulence models by considering the appropriate tuning parameters.

We propose a predictive method for quantifying the structural uncertainties in RANS simulations which does not rely upon calibration data from experimental measurements. Instead, the structural uncertainties are estimated by comparing the results of RANS simulations with the results of direct numerical simulations on a collection of simple geometries with randomly generated features. These DNS results capture most, but not all, of the relevant physical effects found in turbulent flows. Effects such as frame rotation and buoyancy have been ignored, and thus these (small) errors are not accounted for in our results. A statistical model for the structural uncertainty can then be constructed from the results obtained for this collection of random geometries. The random geometries are designed so that the statistical model for the structural uncertainty can be applied to complex geometries.

Rather than treating the model input parameters as random variables, we model the turbulent viscosity predicted by RANS models as a random field. For each random geometry, we use adjoint based inverse modeling to compute the "true" turbulent viscosity field from ensemble averaged DNS results. This differs considerably from previous efforts, which rely on Bayesian inversion to estimate the probability distributions of the turbulence model parameters. Compared to Bayesian inversion, adjoint based inversion is significantly more computationally efficient for such large-scale problems, where the turbulent viscosity at every mesh cell must be determined. The savings afforded by using adjoint based inversion allows us to consider a larger collection of random geometries, thereby allowing a more robust statistical model to be developed. It should be noted that the model uncertainties due to the Boussinesq approximation are ignored. In general, the error in the Reynolds stresses represent a tensor field, while our method, which models the errors in the turbulent viscosity only, represents these errors as a scalar field.

The following sections explain our research efforts in detail. Section 3 describes the method that we have developed for estimating the structural uncertainty in RANS turbulence models. We especially focus on the $k-\omega$ turbulence model due to its popularity in industrial applications. Section 4 presents the initial results obtained for a straight walled channel and randomly generated geometries.

3. Estimating the Structural Uncertainty in RANS Models

The method we have developed consists of two steps: an inverse modeling step and a statistical inference step. The inverse modeling step generates simple random geometries that represent geometric features that are likely to appear in large-scale simulations. Direct numerical simulations are performed on these simple geometries, and an inverse

problem is solved for each geometry to obtain the true turbulent viscosity that accurately reproduces the flow field predicted by direct numerical simulation. The calculated turbulent viscosity fields are stored together with the mean flow field and turbulent properties for a collection of randomly generated geometries. The inverse modeling step reduces the problem of quantifying the sources of uncertainty to a statistical data analysis problem. In this statistical inference step, we analyze the data generated in the inverse modeling step, and build a statistical model of the uncertainty in the calculated RANS turbulence viscosity. The following subsections detail the two proposed steps.

3.1. *Solving the inverse RANS problem using the adjoint method*

The purpose of the inverse RANS modeling is to find the true turbulent viscosity field that produces the most accurate RANS flow solution. Under the assumption that the direct numerical simulation is sufficiently accurate, we use the mean flow field averaged from the direct numerical simulation to calibrate the turbulent viscosity in the RANS simulation.

The inverse RANS problem can be cast as a constrained minimization problem of the form

$$\min_{\mu_t} J \quad \text{s.t.} \quad \mu_t \geq 0. \tag{3.1}$$

The objective function J is defined as

$$J = ||u(\mu_t) - U_{DNS}||^2_{L^2}. \tag{3.2}$$

Here $u(\mu_t)$ corresponds to the RANS flow field produced by a specified turbulent viscosity field μ_t. The flow field U_{DNS} represents the time-average of the flow field predicted by direct numerical simulation. Since the DNS is performed on a three-dimensional mesh, the flow field is also averaged in the spanwise direction so that it can be compared to the two-dimensional RANS results. The initial estimate of μ_t is calculated using a standard $k-\omega$ turbulence model. In the optimization iterations, the turbulent viscosity is decoupled from the transport scalars and is treated as a parameter to be optimized. In each iteration, we essentially solve the Navier-Stokes equations with an additional prescribed (turbulent) viscosity.

The inverse problem given by Eq. 3.1 solves an optimization problem for the turbulent viscosity field μ_t, the dimension of which is equal to the number of cells in the computational mesh. Such high-dimensional numerical optimization problems can only be solved efficiently using a gradient-based algorithm. The adjoint method is an efficient method for computing the required sensitivity gradient. The sensitivity of the objective function J with respect the turbulent viscosity at every mesh cell can be determined by solving a single system of adjoint equations. Compared to methods that use finite differences to compute functional gradients, which require computing a full RANS solution for each mesh cell, the adjoint approach is orders of magnitude more efficient.

Once the sensitivity of the objective function to the turbulent viscosity has been determined, the turbulent viscosity field can be updated to produce a new estimate for the true turbulent viscosity:

$$\log(\mu_t^{k+1}) = \log(\mu_t^k) - \varepsilon \mu_t^k \left.\frac{\partial J}{\partial \mu_t}\right|_{\mu_t^k}. \tag{3.3}$$

A back-tracking line search is used to calculate the step size ε at each iteration. The viscosity field is updated in this manner until the result has converged sufficiently. For each geometry, the resulting optimal turbulent viscosity field μ_t^*, which represents the

true turbulent viscosity field, is stored in a database, together with the RANS flow field $u(\mu_t^*)$.

3.1.1. *The adjoint method for computing the turbulent viscosity in a straight channel*

To demonstrate the validity of our method, we first apply the inverse modeling and statistical inference steps to model the structural uncertainties in a RANS solution of flow through a straight channel. A periodic boundary condition is specified at the channel inlet and outlet. Since the RANS solution is computed at a steady-state, the flow field varies only in the direction normal to the walls. The lower wall is at $y = 0$ and the channel half-width is unity.

For steady incompressible flow through a periodic straight channel, only the x component of velocity (u) is non-zero, and is governed by

$$-\frac{d}{dy}\left(\mu\frac{du}{dy}\right) = f, \tag{3.4}$$

$$u(0) = 0 \qquad \frac{du}{dy}(1) = 0,$$

where $\mu = \mu_t + \mu_\ell$ is the sum of the turbulent and laminar viscosities, and f is the force applied to drive the flow. To determine the corresponding adjoint equations, we first consider the tangent set of equations resulting from substituting $u = \bar{u} + \delta u$ and $\mu = \bar{\mu} + \delta\mu$:

$$\frac{d}{dy}\left(\bar{\mu}\frac{d\delta u}{dy} + \delta\mu\frac{d\bar{u}}{dy}\right) = 0 \tag{3.5}$$

$$\delta u(0) = 0 \qquad \frac{d\delta u}{dy}(1) = 0.$$

For the rest of the derivation, we drop the overbar notation and assume that we are linearized about the states u and μ. The first variation of the objective function J is computed as

$$\delta J = \int_0^1 2(u - U_{DNS})\delta u \; dy. \tag{3.6}$$

Introducing the adjoint velocity $\hat{u}$, we can rewrite Eq. (3.6) as

$$\delta J = \int_0^1 2(u - U_{DNS})\delta u \; dy + \int_0^1 \hat{u}\frac{d}{dy}\left(\mu\frac{d\delta u}{dy} + \delta\mu\frac{du}{dy}\right) dy.$$

Integration by parts gives

$$\begin{aligned}\delta J = \int_0^1 2(u - U_{DNS})\delta u \; dy + \int_0^1 \delta u\frac{d}{dy}\left(\mu\frac{d\hat{u}}{dy}\right) dy - \int_0^1 \delta\mu\frac{du}{dy}\frac{d\hat{u}}{dy}dy \\ + \hat{u}\left(\mu\frac{d\delta u}{dy} + \delta\mu\frac{du}{dy}\right)\Bigg|_0^1 - \mu\frac{d\hat{u}}{dy}\delta u\Bigg|_0^1.\end{aligned}$$

We set all terms involving δu to zero, arriving at the adjoint equation

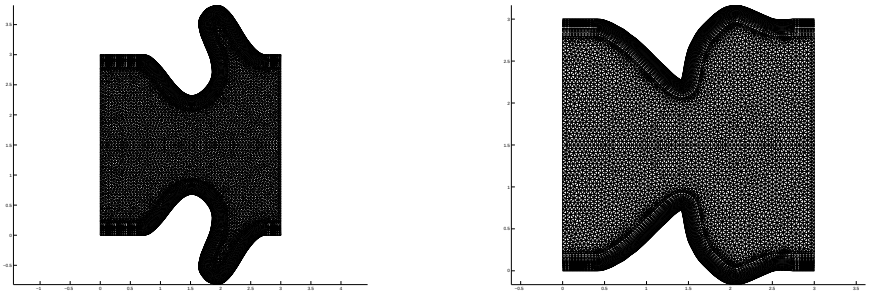

FIGURE 1. Two-dimensional view of randomly generated channel geometries.

$$\frac{d}{dy}\left((\mu_t+\mu_\ell)\frac{d\hat{u}}{dy}\right)=-2\left(u-U_{DNS}\right), \tag{3.7}$$

with corresponding boundary conditions

$$\hat{u}(0)=0 \qquad \frac{d\hat{u}}{dy}(1)=0.$$

The sensitivity of the objective function to the turbulent viscosity can be computed as

$$\frac{\delta J}{\delta \mu_t}=-\frac{d\hat{u}}{dy}\frac{du}{dy}. \tag{3.8}$$

This sensitivity gradient is then used to iteratively optimize the turbulent viscosity field, producing the turbulent viscosity field that minimizes the objective function.

3.1.2. *The adjoint method for computing the turbulent viscosity in a stochastic channel*

To accurately predict the structural uncertainties for turbulent flow around complex geometries, we first solve a RANS inverse problem on a large collection of arbitrary geometries. Because a direct numerical simulation and a RANS inverse problem will be computed on each geometry, the geometries must be sufficiently simple. On the other hand, these geometries should also contain geometric features that are likely to appear in complex engineering geometries, since the statistical model of the structural uncertainty in the turbulent viscosity will be derived from the results obtained on these geometries.

Figure 1 shows a sample of the meshes used in our simulations. Our geometry generator creates channels with randomly shaped lower and upper walls, and the lower and upper walls are symmetric about the channel centerline. A Gaussian process with correlation function $\exp\{-x^2/(c_0^2+c_1|x|)\}$ is simulated using a matrix factorization method (Davis 1987) to produce the randomly oscillating but smooth shapes of the walls. The Gaussian process is conditioned at the two ends so that the end points align with the straight sections of walls. Sharp angles are also created randomly on the lower wall by simulating multiple Gaussian processes. The flows through these randomly generated channels exhibit a variety of flow phenomena that are frequently encountered in engineering simulations, including attached boundary layers under both favorable and adverse pressure gradients, separation on both sharp angles and smooth surfaces, flow recirculation, and flow reattachment on the boundary.

To derive the sensitivity of the objective function with respect to the turbulent vis-

cosity, we start with the tangent set of equations corresponding to steady incompressible flow in a channel with arbitrary geometry:

$$\boldsymbol{u}\cdot\nabla\delta\boldsymbol{u}+\delta\boldsymbol{u}\cdot\nabla\boldsymbol{u}+\nabla\delta p-\nabla\cdot(\delta\mu\nabla\boldsymbol{u})-\nabla\cdot(\mu\nabla\delta\boldsymbol{u})=0, \tag{3.9}$$

$$\nabla\cdot\delta\boldsymbol{u}=0. \tag{3.10}$$

Note that the density is taken to be unity everywhere. We introduce adjoint variables $\hat{\boldsymbol{u}}$ and $\hat{p}$, corresponding to the adjoint velocity and adjoint pressure, respectively. As before, the first variation of the objective function can be written as

$$\delta J=\int_\Omega 2(\boldsymbol{u}-\boldsymbol{U}_{DNS})\cdot\delta\boldsymbol{u}. \tag{3.11}$$

We dot the adjoint velocity $\hat{\boldsymbol{u}}$ into Eq. 3.9, and add the product of the adjoint pressure $\hat{p}$ and Eq. 3.10 to give

$$\begin{aligned}(\boldsymbol{u}\cdot\nabla\delta\boldsymbol{u})\cdot\hat{\boldsymbol{u}}+(\delta\boldsymbol{u}\cdot\nabla\boldsymbol{u})\cdot\hat{\boldsymbol{u}}+(\nabla\delta p)\cdot\boldsymbol{u}\\ -(\nabla\cdot(\delta\mu\nabla\boldsymbol{u}))\cdot\hat{\boldsymbol{u}}-(\nabla\cdot(\mu\nabla\delta\boldsymbol{u}))\cdot\hat{\boldsymbol{u}}+\hat{p}(\nabla\cdot\delta\boldsymbol{u})=0.\end{aligned}$$

Integrating by parts over the domain and adding the result to Eq. 3.11 gives

$$\begin{aligned}\delta J=&\int_\Omega 2(\boldsymbol{u}-\boldsymbol{U}_{DNS})\cdot\delta\boldsymbol{u}+\int_\Omega d\mu\nabla\boldsymbol{u}:\nabla\hat{\boldsymbol{u}}\\ &+\int_\Omega\left[\delta\boldsymbol{u}\cdot(-\boldsymbol{u}\cdot\nabla\hat{\boldsymbol{u}}+\nabla u\cdot\hat{\boldsymbol{u}}-\mu\nabla^2\hat{\boldsymbol{u}}+\nabla\hat{p})-\delta p\nabla\cdot\hat{\boldsymbol{u}}\right]\\ &+\int_{\partial\Omega}\left[\delta p(\hat{\boldsymbol{u}}\cdot\vec{n}-\mu((\nabla\delta\boldsymbol{u})\cdot\hat{\boldsymbol{u}})\cdot\vec{n}-\delta\mu((\nabla u)\cdot\hat{u})\cdot\vec{n}\right].\end{aligned}$$

Finally, we set all terms involving $\delta\boldsymbol{u}$ or δp to zero to obtain Eqs. 3.12 and 3.13.

$$-\hat{\boldsymbol{u}}\cdot\nabla\boldsymbol{u}+\boldsymbol{u}\cdot\nabla\hat{\boldsymbol{u}}+\nabla\cdot((\mu_\ell+\mu_t)\nabla\hat{\boldsymbol{u}})-\nabla\hat{p}=-2(\boldsymbol{u}-\boldsymbol{U}_{DNS}) \tag{3.12}$$

$$\nabla\cdot\hat{\boldsymbol{u}}=0. \tag{3.13}$$

The adjoint velocity must also satisfy the adjoint boundary condition

$$\hat{\boldsymbol{u}}(x)=0,\quad x\in\partial\Omega. \tag{3.14}$$

The sensitivity of the objective function can then be calculated as

$$\frac{\delta J}{\delta\mu_t}=\nabla\hat{\boldsymbol{u}}:\nabla\boldsymbol{u}. \tag{3.15}$$

As before, this sensitivity gradient is used to update the turbulent viscosity field until the magnitude of the objective function has decreased sufficiently.

3.2. *Statistical modeling of the turbulent viscosity field*

The inverse modeling step computes the true turbulent viscosity by inverting an averaged direct numerical simulation flow field for randomly generated geometries. These true turbulent viscosity fields are stored together with the flow fields and turbulent properties. The inverse modeling step reduces the uncertainty quantification problem to a statistical data analysis problem. The statistical inference step uses the data generated by the first

step to fit a statistical model of the relation between the true turbulent viscosity, the flow field and the turbulent properties.

In developing the statistical model, we quantify the dependence of the magnitude of uncertainty and the correlation length of the random field as a function of various metrics such as the Reynolds number, geometric length, distance to wall, local velocity strain rate and rate of rotation. The statistical model built in this step provides a full characterization of a random field, which can be sampled on an arbitrary geometry. Each sample of the random field provides a deterministic relation between the turbulent viscosity μ_t, the flow field, and the transport properties.

In engineering applications, the sources of uncertainties must be propagated to the quantities of interest of a RANS simulation, such as aerodynamic forces and moments. To validate our statistical model against experimental data, the modeled uncertainties must be propagated to the quantities measured in experiments, such as pressure and wall stress. Because we model the sources of uncertainties as a random field, the stochastic dimension of the uncertainty propagation problem can be very high, especially when the size of the computational domain is significantly larger than the correlation length of the random field. Due to this high-dimensionality, we use the Monte Carlo method for propagating uncertainties. For example, in validating our statistical model against experimental data, we may only need to determine whether the experimental data lie within the error bars caused by the uncertainties. In such cases, an estimate for the standard deviation with moderate accuracy is sufficient. Monte Carlo methods, which have the advantage of being insensitive to the stochastic dimension, are thus suitable for such cases.

4. Results

4.1. *Turbulent flow in a straight channel*

For the straight channel, we consider flow at a friction Reynolds number of 180 based on the channel half-width and friction velocity. The direct numerical simulation results were taken from Moser, et al. (Moser 1999). Figure 2 shows the results of the adjoint optimization routine. The left figure shows the velocity profiles plotted versus the wall-normal distance determined DNS. Note that the DNS result plotted in the left figure depicts the time-averaged velocity profile. The figure on the right shows the error between the DNS result and the initial RANS velocity profile, as well as the error between the DNS and optimized profile. The initial velocity profile predicted using the $k-\omega$ model differs significantly from the profile predicted by direct numerical simulation, with a maximum error of approximately 1.2. After 1000 optimization iterations, the maximum error has decreased to a value of approximately 0.05.

The resulting turbulent viscosity field is also plotted in Figure 2. Although direct numerical simulation does not involve explicitly calculating a turbulent viscosity, an effective turbulent viscosity can be determined by considering a force balance in the channel. We observe that the optimized turbulent viscosity moves towards the "effective" turbulent viscosity as the optimization proceeds. The optimized turbulent viscosity is nearly identical to the "effective" viscosity near the wall, where changes in viscosity have the largest global impact on the velocity profile.

The optimized true turbulent viscosity profile (μ_t^*) can be used to model the error in the turbulent viscosity field predicted by the RANS model. We first calculate σ_μ as

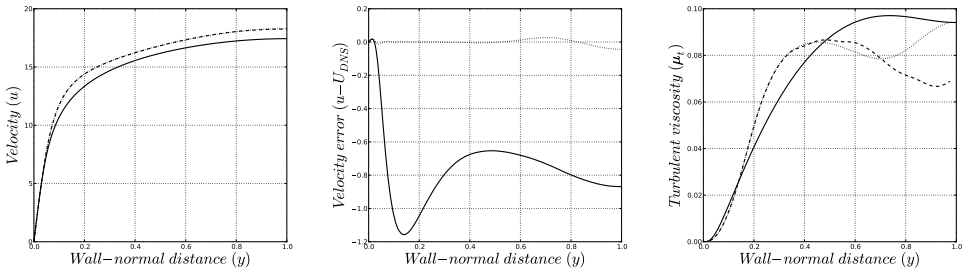

FIGURE 2. Velocity, velocity error, and corrected turbulent viscosity: ——— initial profile; ····· profile after 1000 adjoint optimization iterations; - - - - DNS

$$\sigma_\mu = \text{stdev}\left(\log\left(\frac{\mu_t^*}{\mu_t^0}\right)\right). \tag{4.1}$$

The turbulent viscosity field μ_t^0 represents the turbulent viscosity predicted by the $k-\omega$ turbulence model, namely $\mu_t^0 = k/\omega$. In our formulation, the error factor is modeled as a universal constant, and thus models the error in the RANS solution at any Reynolds number. The value of σ_μ was determined by considering flow at a single friction Reynolds number, namely $Re_\tau = 180$. The inverse problem is solved only once, and the resulting value of σ_μ is used to propagate the uncertainty in channel flows at other friction Reynolds numbers.

To propagate the uncertainty predicted using our method, we use the Monte Carlo method. For each Monte Carlo simulation, we obtain a sample turbulent viscosity field μ_t^s according to $\mu_t^s = e_\mu\ \mu_t^0$. The error factor e_μ for the turbulent viscosity is sampled from a log-normal distribution, namely

$$e_\mu = \exp(\mathcal{N}(0, \sigma_\mu^2)), \tag{4.2}$$

where $\mathcal{N}(0, \sigma_\mu^2)$ is a normally distributed random variable with zero mean and standard deviation σ_μ. Sampling from a log-normal distribution ensures that this error factor will be nonnegative, and thus the sampled turbulent viscosity field μ_t^s will also be nonnegative. We then compute a RANS solution for each sample with the prescribed turbulent viscosity field μ_t^s. The results from each Monte Carlo simulation are stored, and a mean profile and standard deviation can be calculated from these results.

Figures 3 and 4 show the results for three different friction Reynolds numbers, $Re_\tau =$ 180, 395, and 590. For each case, 20 Monte Carlo samples were used to estimate the mean profile and standard deviation. Figure 3 shows four of the sample velocity profiles at each of the friction Reynolds numbers considered.

We note that the direct numerical simulation results are typically within the two standard deviation bounds.

4.2. *Initial Results for Turbulent Flow in a Stochastic Channel*

For each randomly generated geometry, a direct numerical simulation was performed with a mesh size of around 1.5 million cells. Because both the small-scale vortices near the wall and the large-scale vortices due to flow separation must be resolved, a significant number of grid points are required in the spanwise direction. The meshes consist of a structured boundary layer mesh near the lower wall, and an unstructured simplex mesh

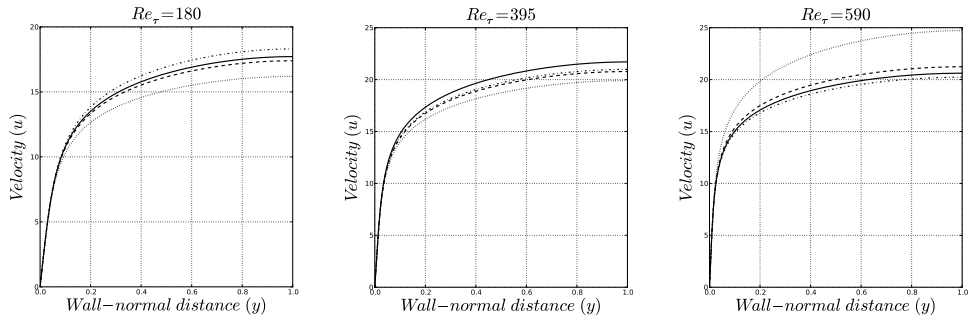

FIGURE 3. Monte Carlo sample velocity profiles at $Re_\tau = 180$, $Re_\tau = 395$, and $Re_\tau = 590$.

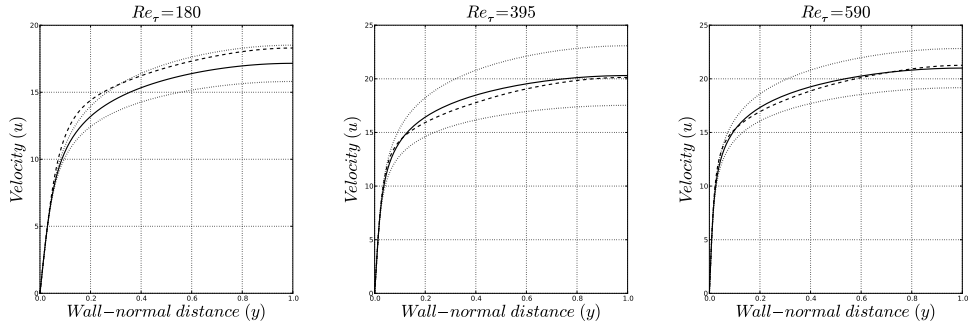

FIGURE 4. Profiles for channel flow at $Re_\tau = 180$, $Re_\tau = 395$, and $Re_\tau = 590$: ——— mean profile; ····· +/− two standard deviations; – – – – DNS

in the remainder of the domain. The two-dimensional meshes shown in Figure 1 were extruded in the spanwise direction to create the fully three-dimensional meshes required to capture the turbulent structures that appear in direct numerical simulation.

The CDP solver, developed at the Center for Turbulence Research at Stanford University, was used to perform the direct numerical simulations (Ham 2007; Ham 2008; Mahesh 2004). The Joe solver, which was also developed at the Center for Turbulence Research, was used to obtain the RANS solutions. No-slip boundary conditions are applied to the randomly shaped lower and upper walls. The left and right vertical boundaries are connected using a periodic boundary condition. Periodic boundary conditions are also applied in the spanwise direction. For each geometry, a constant forcing is applied everywhere in the flow in the direction parallel to the channel centerline. The forcing was chosen to produce a friction Reynolds number (based on channel half-width and friction velocity) of 180 for a straight-walled periodic channel with the same inlet height as the random geometry channels. The turbulent flow field calculated by direct numerical simulation is averaged both in time and in spanwise direction to estimate the mean flow field. The mean flow field is then stored for use in the RANS inverse problem.

Figure 5 shows a comparison between the RANS and DNS results. We note that the x-velocity component along the channel centerline predicted by RANS is larger than that predicted by direct numerical simulation in both cases shown in Figure 5, and this discrepancy is present in almost all other geometries. The relative errors in the velocity at the centerline are typically on the order of 15-20%. These initial results suggest that the true turbulent viscosity field computed using the adjoint method will differ from

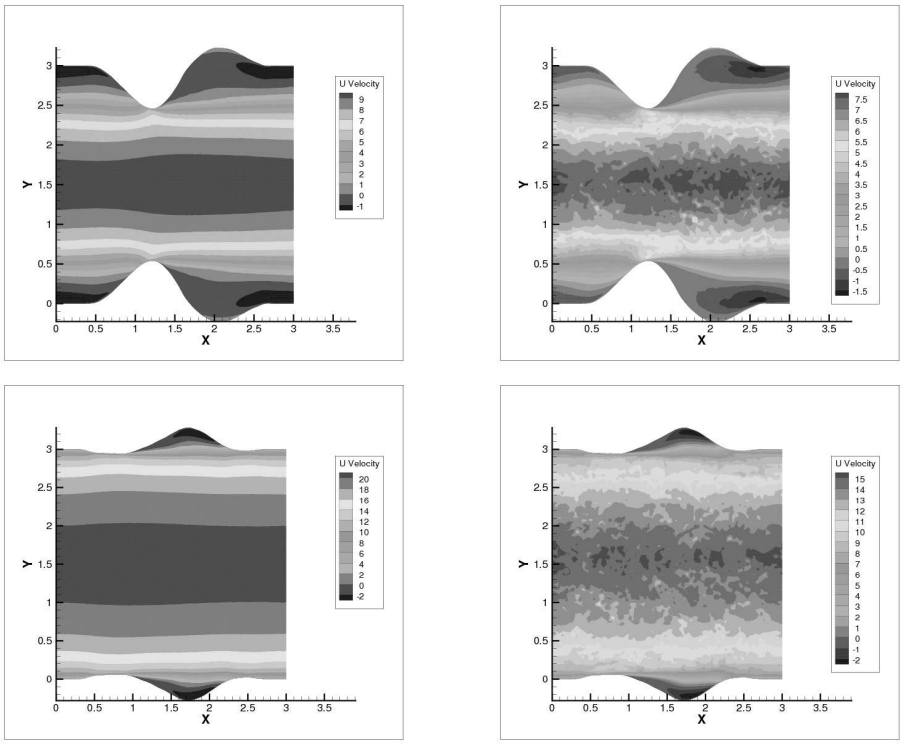

FIGURE 5. x-velocity contours predicted by RANS and DNS for two sample geometries; The RANS results are plotted on the left, and the DNS on the right.

that predicted using RANS. We are currently developing the continuous adjoint solver that will allow us to solve the inverse problem. Once this has been completed we will be able to construct a statistical model for the structural uncertainties in flow through a stochastic channel.

5. Conclusions

The proposed method has shown promising results for turbulent flows in a straight-walled channel. We have successfully applied adjoint optimization to solve an inverse problem for the turbulent viscosity field that produces the most accurate flow solution relative to the results obtained using direct numerical simulation. We have also developed a statistical model for the structural uncertainties in flow through a straight channel. Extending our method should be straightforward for the collection of randomly generated geometries. Once these results have been obtained, we will be able to provide estimates for the structural uncertainties in RANS simulations of turbulent flow.

REFERENCES

DAVIS, D. & SLIMON, S. 2004 Practical error assessment for RANS-based drag prediction. AIAA Paper 2004-4956.

DAVIS, M.W. 1987 Production of conditional simulations via the LU triangular decomposition of the covariance matrix. *Math. Geol.* **19**, 91–98.

Ham, F. 2008 Improved scalar transport for unstructured finite volume methods using grids based on simplex superposition. In *Center for Turbulence Research, Annual Briefs, Stanford University*.

Ham, F., Mattsson, K., Iaccarino, G., Moin, P. 2007 Towards time-stable and accurate LES on unstructured grids. In *Complex Effects in Large Eddy Simulation, Lecture Notes in Computational Science and Engineering 56*, 235–249.

Loeven, G. & Bijl, H. 2009 Probabilistic collocation used in a two-step approach for efficient uncertainty quantification in computational fluid dynamics prediction. *CMES: Computer Modeling in Engineering & Sciences* **36** (2), 193–212.

Mahesh, k., Constantinescu, G., & Moin, P. 1999 A numerical method for large-eddy simulation in complex geometries. *J. Comput. Phys.* **197**, 215–240.

Moser, R., Kim, J., & Mansour, N. 1999 DNS of turbulent channel flow up to $Re_\tau = 590$. *Phys. Fluids* **11** (4), 943–945.

Oliver, T., & Moser, R. 2009 Uncertainty quantification for RANS turbulence model predictions. In *American Physical Society, 62nd Annual Meeting of the APS Division of Fluid Dynamics*.

Vaughn, M., & Chen, C. 2007 Error versus $y+$ for three turbulence models: Incompressible flow over a unit flat plate. AIAA Paper 2007-3968.

Wild, J. 2007 Validation of numerical optimization of high-lift multi-element airfoils based on Navier-Stokes-equations. AIAA Paper 2007-2939.

Witteveen, J., Doostan, A., Pecnik, R., & Iaccarino, G. 2009 Uncertainty quantification of the transonic flow around the RAE 2822 airfoil. In *Center for Turbulence Research, Annual Briefs, Stanford University*.